

CRYSTAL STRUCTURE PARAMETERS AS PREDICTORS OF VNIR SPECTROSCOPY OF SYNTHETIC PYROXENES. Samantha E. Peel¹, M. Darby Dyar¹, and Rachel L. Klima². ¹Dept. of Astronomy, Mount Holyoke College, South Hadley, MA 01075, peel20s@mtholyoke.edu; ²Johns Hopkins University, Applied Physics Laboratory, Laurel MD, 20723.

Introduction: Pyroxenes are among the most common minerals in the solar system and are ideally suited for remote geochemical analysis because their distinctive spectra are sensitive to mineral composition. Spectral features arising from pyroxene have long been recognized in remote telescopic and orbital data. Fe²⁺ in the M1 site gives rise to bands at 1 and 1.2 μm, and Fe²⁺ in M2 to 1 and 2 μm bands. Other cations such as Ca²⁺ have effects on pyroxene spectra because they change the lattice parameters of the crystal structure and thus the crystal field splitting energies of the

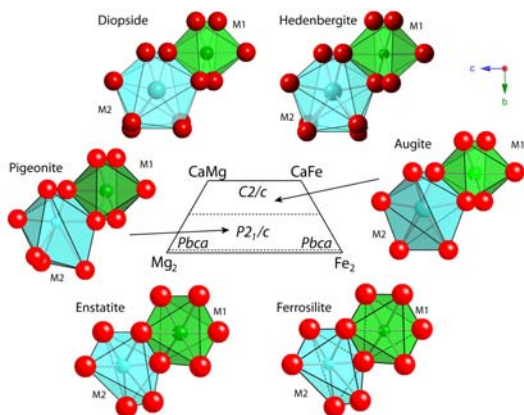


Fig. 1. Configurations of the M1 and M2 polyhedra in different space groups within the pyroxene quadrilateral, viewed down the *a* axis, with *c* horizontal and *b* vertical.

Fe cations (Fig. 1). Work dating back to the 1970's [1] demonstrated a fundamental relationship between composition and energy of the pyroxene bands. Thus, there should be a predictable relationship between crystal structure parameters and band energies. We here investigate relationships between steric parameters of the pyroxene structure and the intensity and position of bands at 1.0, 1.2, and 2 μm in the near-IR.

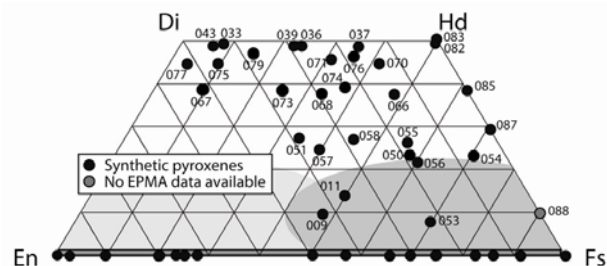


Fig. 2. Pyroxene quadrilateral showing compositions of samples used in this study, which were synthesized in the laboratory of Donald Lindsley at Stony Brook University.

Methods: Spectra of synthetic pyroxenes covering the Fe-Mg-Ca quadrilateral in 5-10 mol% increments were used [3-5] (Fig. 2). The Modified Gaussian Model was used to deconvolve their spectra into component absorption bands, which were compared against results of single crystal structure refinements (SREF) of pyroxenes with the same chemical compositions, acquired from the American Mineralogist Crystal Structure Database. For each structure, several characteristics of the Fe polyhedra were tabulated for M1 and M2 sites (Table 1). These were then compared to positions and intensities of spectral features for samples where both SREF and spectral data were available.

1. O3-O3-O3 bond angle	
2. Mean octahedral quadratic elongation (λ)	$\lambda_{M1} = \sum_{i=1}^6 \left(\frac{l_i}{l_0}\right)^2 / 6$
3. Angular Variance (σ)	$\sigma_{M2} = \sum_{i=1}^{12} (\theta_i - \theta_{avg})^2 / 11$
4. O3-O3 distance between M2 sites	
5. O3-M2-O3 bond angles	
6. O1-M1-O1 bond angles	
7. O1-M2-O1	
8. O1-O1 distance between M1 sites	
9. O1-O1 along edges between M1 and M2 sites	
10. O2-M1-O2 bond angle	
11. Mean bond length	

Results: Of the structure parameters considered, some were more useful for predicting band positions than others. The λ value of the M2 site is an excellent predictor of the energies of the 1 and 2 μm but not the 1.2 μm bands (Fig. 3). However, λ_{M1} plotted against band energy shows a similar trend, probably because the two sites are so intimately related (Fig. 4). In the pyroxene single-chain structure, M2 sites share 1 of 12 edges with adjacent M1 sites and 2 edges with other M2's; the M1 sites share 3 of 12 edges, all with M2. Many other structure parameters also correlate with the energies of the 1 and 2 μm bands. For example, the σ_{θ} of the M1 site correlates positively with 1 and 2 μm band positions, and not with 1.2 μm. The O1-M1-O1, O1-M2-O1, and O3-M1-O3 bond angles all show correlations with 1 and 2 μm band positions.

Perhaps because the 1.2 μm band is significantly weaker, correlations of structure parameters with its position are not as clear-cut. Even when data from samples for which VNIR data are not available are

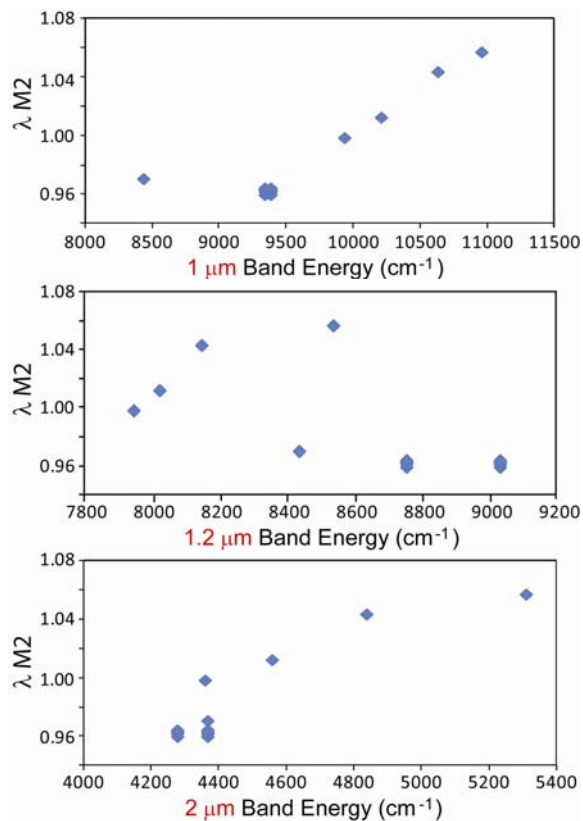


Fig. 2. Band energy of 1 (top), 1.2 (middle) and 2 μm (bottom) bands plotted against λ of the M2 site. Fe^{2+} in the M2 site gives rise to absorptions at 1 and 2 μm but not at 1.2 μm , so the lack of trend for 1.2 μm is expected.

included, there is only the suggestion of a trend with the O1(a)-M1-O1(c) bond angle (Fig. 5).

Discussion: Changes in peak positions of 1 and 2 μm bands with space group were known to be conspicuous [5]. This study shows that many of the structure parameters for pyroxenes also vary in systematic ways with the energies of these bands. These results show that variations in individual polyhedral shapes cause structural changes throughout the pyroxene structure. Data suggest that the approach of using crystal structure parameters to predict pyroxene band positions is as predicted by crystal field theory quite promising. We are pursuing acquisition of SREF data on all samples in our suite of synthetic samples to enlarge our data set. Because pyroxene crystal structures can be predicted from compositions [6], *ab initio* calculations [e.g. 7] based on our SREF results should eventually make it possible to confidently predict band positions on the basis of pyroxene chemistries and vice versa.

Finally, it is interesting to note variations in structure parameters in samples with the same compositions from other studies (vertical groups in Fig. 4). These data reflect differences in cooling histories of synthetic samples, and serve as a reminder that structure parameters of samples with identical compositions can be

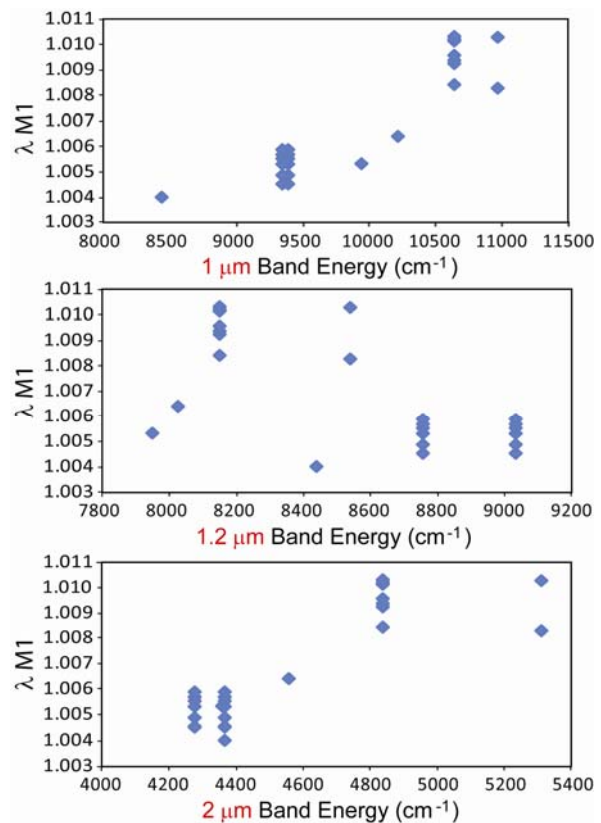


Fig. 3. Band energy of 1 (top), 1.2 (middle) and 2 μm (bottom) bands plotted against λ of the M1 site. The relationship between 2 μm band energy and M1 distortion shows the interrelationships of the two sites, which share edges.

highly variable as a function of cooling history, and thus will also have different band positions.

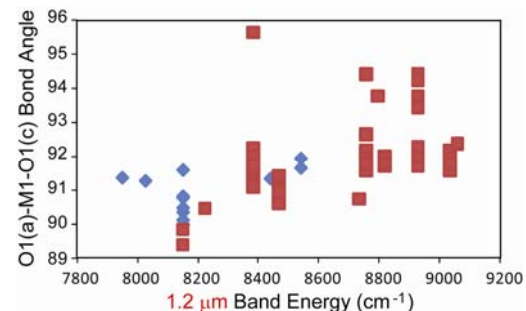


Fig. 4. O1(a)-M1-O1(c) angles plotted against the 1.2 μm band. Samples for which SREF and VNIR measurements were done on the exact same samples are shown in blue as in other figures; red squares are SREF data from synthetic pyroxenes other than those in our VNIR study.

Acknowledgments: This project was supported by NASA LASER grant NNX09AM66G.

References: [1] Adams J. B. (1974) *JGR*, 79, 4829-4836. [2] Hazen R. M. et al. (1978) *Proc. LPSC*, 9th, 2919-2934. [3] Klima R. L. et al. (2007) *MAPS*, 42, 235-253. [4] Klima R. L. et al. (2008) *MAPS*, 43, 1591-1604. [5] Klima R. L. et al. (2011) *MAPS*, in press. [6] Thompson, R. M. and Downs, R. T. (2003) *Am. Mineral.*, 88, 653-666. [7] Valenzano, L. et al. (2009) *Phys. Chem. Minerals*, 36, 415-420.